

# A Branch-and-Bound Algorithm for the Close-Enough Traveling Salesman Problem

Walton Pereira Coutinho, Anand Subramanian

Departamento de Engenharia de Produção, Centro de Tecnologia — Universidade Federal da Paraíba  
Campus I, Bloco G, Cidade Universitária, 58051-970, João Pessoa - PB, Brazil  
walton@ct.ufpb.br, anand@ct.ufpb.br

Roberto Quirino do Nascimento

Departamento de Computação Científica, Centro de Informática — Universidade Federal da Paraíba  
Campus I, Bloco G, Cidade Universitária, 58051-970, João Pessoa - PB, Brazil  
roberto@ci.ufpb.br

Artur Alves Pessoa

Departamento de Engenharia de Produção — Universidade Federal Fluminense  
Rua Passo da Pátria, 156, Bloco E, 4 andar, São Domingos, 24210-240, Niterói - RJ, Brazil  
artur@producao.uff.br

This paper deals with the Close-Enough Traveling Salesman Problem (CETSP). In the CETSP, rather than visiting the vertex (customer) itself, the salesman must visit a specific region containing such vertex. To solve this problem, we propose a simple yet effective exact algorithm, based on Branch-and-Bound and Second Order Cone Programming (SOCP). The proposed algorithm was tested in 824 instances suggested in the literature. Optimal solutions are obtained for open problems with up to a thousand vertices. We consider both instances in the two- and three-dimensional space.

*Key words:* close-enough traveling salesman problem; branch-and-bound; second order cone programming

## 1. Introduction

The Traveling Salesman Problem (TSP) has been widely studied over the last decades. In the symmetric TSP one aims to find a shortest *Hamiltonian Cycle* in a complete and undirected graph  $G = (V, E)$ , where  $V$  is the set of vertices (customers) and  $E$  is the set of edges connecting the vertices. The length of each edge is given by a previously determined metric, for example, the *Euclidean* distance between two vertices  $p$  and  $q \in V$  that can be defined as  $d_{pq} = \|\mathbf{v}^p - \mathbf{v}^q\|_2$ , where  $\mathbf{v}^p$  and  $\mathbf{v}^q$  denote the respective coordinate vectors of  $p$  and  $q$  and  $\|\cdot\|_2$  the Euclidean norm. Due to the importance and applicability of the TSP, a large number of variants and numerical algorithms to compute exact and approximate solutions for these problems were proposed in the literature. More information about the TSP can be found, e.g., in the book of Applegate et al. (2011).

The Close-Enough Traveling Salesman Problem (CETSP) is a generalization of the TSP and can be cast, according to Mennell (2009), as a particular case of three other TSP-related problems: The Traveling Salesman Problem with Neighborhoods (TSPN) (Arkin and Hassin 1994), the Generalized Traveling Salesman Problem (Silberholz and Golden 2007) and the Covering Tour

Problem (Gendreau et al. 1997). In the CETSP, rather than visiting the vertex (*customer*) itself, the salesman must visit a specific region containing such vertex. In this paper we will assume that the covering regions are circles. This is a classical assumption in the CETSP literature. Therefore the vertex  $i \in V = \{1, \dots, n\}$  is considered to be covered if the salesman passes through the disc  $D_i$  with radius  $r_i$  containing the vertex  $i$  or at least touches the border of this disc. In a three-dimensional space the regions are considered to be spheres and, in the same sense, the vertices are considered covered if the salesman passes through or at least touches the border of their respective covering spheres.

The CETSP can be formally described as follows. We are given a set of vertices  $V = \{0, \dots, n\}$  in a bi-dimensional space and its coordinates  $(\bar{x}_i, \bar{y}_i)$ ,  $i = 0, \dots, n$ . Each vertex  $i$  is covered by a circle  $\mathcal{D}_i$  with radius  $r_i$ . We assume that  $(\bar{x}_i, \bar{y}_i) \neq (\bar{x}_j, \bar{y}_j)$ ,  $\forall i, j \in V$ ,  $i \neq j$ , i.e., there is no overlapping between the vertices. The problem lies in determining the value of the coordinates of the *hitting points*  $(x_i, y_i) \in \mathbb{R}^2$ ,  $i = 0, \dots, n$ , a.k.a. *representative points* (Mennell 2009), and a sequence  $\mathcal{S} = \{k_0, k_1, \dots, k_n\}$  such that the tour over these coordinates form a *Hamiltonian Cycle* of minimum length and  $(x_i, y_i) \in \mathcal{D}_i$ ,  $\forall i \in V$ . In the example of Figure 1, the tour “hits” the circle associated to vertices 1 and 3 only in a single point, whereas for the vertex 2, the tour “hits” its associated circle in an infinite number of points. Here we denote the vertex  $i = 0$  representing the depot and we assume that  $\mathcal{D}_0$  is a circle with  $r_0 = 0$ . This definition can be easily extended to the three-dimensional space by using three coordinates, that is  $(\bar{x}_i, \bar{y}_i, \bar{z}_i)$ , instead of two.

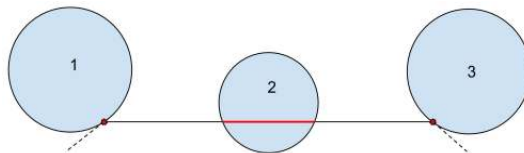
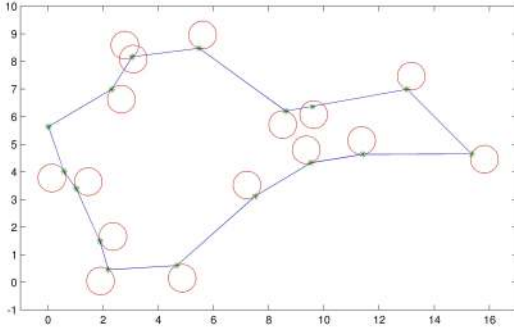


**Figure 1** Example of hitting points

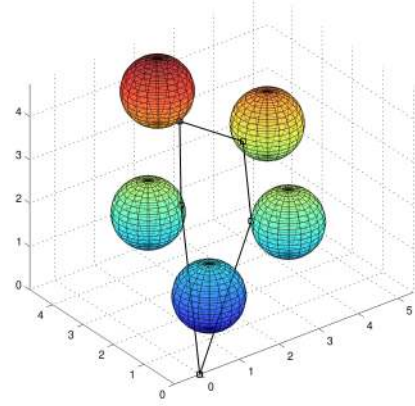
When there is only a single hitting point in a circle, then such point is called *turn point*. It can be shown that the number of turn points in a feasible CETSP solution can be smaller than  $n$  (Behdani and Smith 2013).

Figure 2 illustrates an example of a CETSP solution in the two-dimensional space, whereas Figure 3 depicts a CETSP solution in the three-dimensional space.

The CETSP has several applications in real-world problems. For example, by using Radio Frequency Identification (RFID) tags connected to physical meters one can encode the identification number of the meter and its current reading into digital signals. This way, an utility truck equipped with an Automatic Meter Reading (AMR) system can remotely collect and transmit data from a certain distance. Hence, in the AMR context, the meter reader is not required to personally visit



**Figure 2** Feasible solution for the CETSP in  $\mathbb{R}^2$



**Figure 3** Feasible solution for the CETSP in  $\mathbb{R}^3$

each customer, but only get within a certain radius of every customer (Gulczynski et al. 2006, Dong et al. 2007).

Unmanned Aerial Vehicles (UAVs) have been widely used for military and civil missions, especially when the presence of an human crew on board become too dangerous. As examples of the use of UAVs we can cite Aerial Reconnaissance, Aerial Forest Fire Detection, Ship Tracking, Supply Delivering (food, munition) to targets, Geographic Region Monitoring and Surveillance of Pipelines. If the UAV is equipped with a sensor, the vehicle can operate successfully from a certain distance to the target. Another example occurs when the UAV needs just to drop its cargo as close as possible to the target locations, like in special military operations. These are all practical applications that can be modeled as a CETSP.

Recently, Behdani and Smith (2013) pointed out that there is a lack of exact algorithms for solving the CETSP. Moreover, Mennell et al. (2011) highlights that developing lower bounds for the CETSP is a non-trivial task. To the best of our knowledge, the present work is the first one to present a method that yields exact optimal solutions for the CETSP. More specifically, we propose a simple yet effective combinatorial branch-and-bound algorithm, in which the subproblem is based on a Second-Order Cone Programming (SOCP) formulation (Lobo et al. 1998, Farid and Goldfarb 2003, Boyd and Vandenberghe 2004), that is capable of solving instances with up to a thousand nodes. Moreover, our method was also designed to deal with instances both in two- and three-dimensional spaces.

The remainder of this paper is organized as follows. Section 2 contains the related work. Section 3 describes the proposed branch-and-bound approach. Computational results are provided in Section 4. Finally, Section 5 presents the concluding remarks of this work.

## 2. Related work

In this section we provide a brief outline of the solution approaches proposed for solving the CETSP and some of its related variants.

With a view of obtaining near-optimal solutions, several heuristics have been developed for the CETSP. Gulczynski et al. (2006) and Dong et al. (2007) proposed several heuristic methods for the case where all regions discs have the same radius. Their methods are based on the concept of *supernodes*. A feasible *supernode* set  $S$  is defined as the set of points in  $\mathbb{R}^2$ , including the depot, such that each vertex  $v_i \in V$ ,  $i = 1, \dots, n$ , is within  $r$  units of at least one point  $S$ . The heuristics were based on three distinct phases: (i) generation of the *supernode* set; (ii) construction of the tour over the *supernode* set; and (iii) improvement of the tour by moving the *supernodes*. Although the heuristics share the same main structure, the procedures adopted in each phase differ from each other.

Yuan et al. (2007) dealt with the Optimal Robot Routing Problem (ORRP) as a TSPN where the compact sets covering the vertices are disjoint discs with a given radius. The ORRP consists in designing the optimal route of a mobile robot operating in a wireless sensor network in such a way that the robot can collect data from all sensors while minimizing the total distance traveled. Hence, this problem may be cast as a particular CETSP instance where the discs representing the action area are all disjoint. The authors proposed a two-phase algorithm for the TSPN, by decomposing the TSPN into a combinatorial problem and a continuous optimization problem. The former aims to find a near-optimal solution for the TSP over the original vertices, whereas the latter is based on an Evolutionary Algorithm that applies search space reduction techniques to find the *hitting points*.

On the bases of preliminary results in Mennell (2009), Mennell et al. (2011) put forward a *Steiner Zone Heuristic* based on three phases. The first one is the so-called *Graph Reduction*, where the total number of vertices is reduced to a smaller number of *Steiner Zones*. The second one is the *Tour Finding*, where a TSP tour is built over *supernodes* selected from each *Steiner Zone*. In the last phase, denoted as *Tour Improvement*, exact and heuristic approaches are applied to shorten the tour length.

Behdani and Smith (2013) proposed two different partitioning schemes to approximate the continuous covering regions. One of them is the so-called *grid-based* discretization, which approximates arbitrary covering regions by rectangles. The other one is the so-called *arc-based* partitioning scheme, first intended for circular covering regions, which discretizes the border of the circles into possible *hitting points*. Moreover, the authors devised a Mixed Integer Programming (MIP) approach, based on three mathematical formulations and on Benders decomposition, that was capable of finding tight lower and upper bounds for instances with up to 21 nodes. The main characteristic of this approach is that the more the partitioning scheme approximates the circular regions the more solutions converge to the actual optimal solution. On the other hand, high partitioning levels make the method prohibitively expensive in terms of computing time.

More recently, Hà et al. (2013) studied a CETSP variant called Close Enough Arc Routing Problem (CEARP). In the CEARP there is a predefined directed graph  $G = (V, A)$ , where  $V = \{v_0, v_1, \dots, v_{n-1}\}$  is the set of vertices and  $A = \{(v_i, v_j) \mid v_i, v_j \in V\}$  is the set of arcs connecting this vertices, and another set of vertices in  $\mathbb{R}^2$ , representing the customers and denoted by  $W = \{w_1, w_2, \dots, w_l\}$ , that must be covered. The CEARP consists in finding a minimum-cost cycle over the graph  $G$  such that every customer in  $W$  is covered, i.e., lies within a certain distance from any arc of the cycle. This problems fits exactly in the AMR context, and it was originally called *CETSP over a street network* by Shuttleworth et al. (2008), since in their approach the arcs of the graph are associated to streets.

### 3. Branch-and-Bound algorithm

This section presents a complete description of the proposed combinatorial branch-and-bound algorithm for the CETSP.

In summary, the method is as follows. Each branch-and-bound node is associated to an optimal partial tour that needs to visit only a given subset of vertices in a particular order. At the root node, the algorithm chooses three vertices in order to generate an initial sequence (see Section 3.2). Since there are only three vertices involved in this sequence and costs are symmetric, their order will not affect the solution. Therefore, this partial tour is a valid relaxation of the main problem. The problem of choosing the exact coordinates of the tour to be visited, given a predefined sequence, can be formulated as a Second Order Cone Programming (SOCP) problem (see Section 3.1). If the associated solution is feasible (see Section 3.3), i.e., all customers are covered, then this solution is optimal and the problem is solved. Otherwise, the algorithm branches into three subproblems, where in each of them, a vertex that does not belong to the tour is inserted in a different position (see Section 3.4). A node is pruned if its cost is greater than or equal to the best known upper bound or if its associated solution is feasible. Otherwise, a branching is performed over this node using the same rationale applied in the root node.

Figure 4 shows an example of the execution of the method for an instance involving 7 vertices. The set of uncovered vertices is represented by a list alongside its correspondent node, whereas the bold numbers represent the chosen vertices to be inserted. In this case, the relaxed solution found at the root node was  $0 \rightarrow 3 \rightarrow 6 \rightarrow 0$ . Next, the vertex 1 was selected to be inserted in every possible position, thus resulting in three child nodes. When inserting vertex 1 in the first or in the second position of the tour it can be verified that vertex 4 is covered, but the same does not happen when vertex 1 is inserted in the third position because vertex 4 still remains uncovered. Branchings are then performed as long as they are necessary. This particular example depicts a possible branch-and-bound tree associated to this 7-vertices instance. Prunings by bound were

not considered for the sake of simplicity. As indicated in the figure, the optimal solution of this instance is  $0 \rightarrow 3 \rightarrow 1 \rightarrow 6 \rightarrow 5 \rightarrow 0$ .

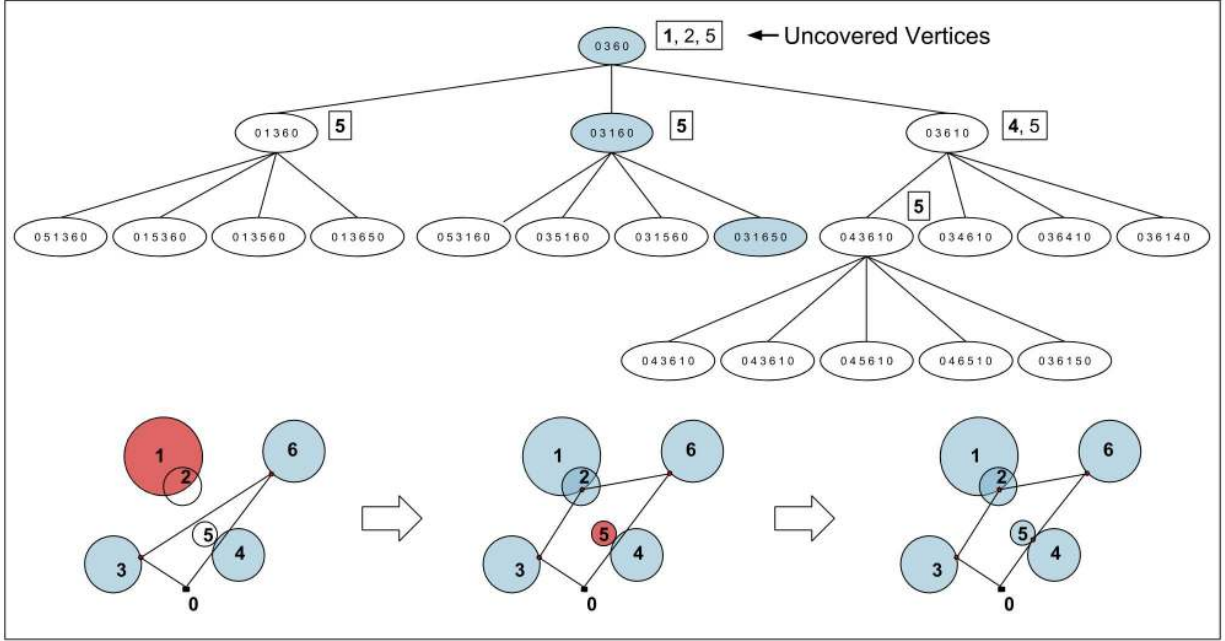


Figure 4 Example of the proposed branch-and-bound algorithm for an instance with 7 vertices

It can be noticed that the maximum number of nodes in a certain level  $l$  of the branch-and-bound tree is given by  $\frac{(l+2)!}{2}$ . Moreover, in the worst case, the total number of nodes corresponds to  $\sum_{l=0}^n \frac{(l+2)!}{2} = \mathcal{O}(n+2)!$ .

### 3.1. Second-Order Cone Formulation

In this section we provide a mathematical formulation, based on SOCP, for solving the branch-and-bound subproblems. This formulation has been initially proposed by Mennell (2009) for the Touring Steiner Zones Problem when the sequence of visits is given.

Let  $\mathcal{S} = \{i_0, \dots, i_q\}$ ,  $q < n$ , be any partial sequence found during the execution of the branch-and-bound algorithm. The subproblems of the branch-and-bound consist in finding the values of the *hitting points* coordinates  $(x_{i_k}, y_{i_k})$ ,  $k = 0, \dots, q$ , such that the length of the partial tour is minimized. Let us assume that  $i_{-1} = i_q$ . The formulation is as follows.

$$\min \sum_{k=0}^q z_k \tag{1}$$

$$\text{s.t. } w_k = x_{i_{k-1}} - x_{i_k}, \quad k = 0, \dots, q \tag{2}$$

$$u_k = y_{i_{k-1}} - y_{i_k}, \quad k = 0, \dots, q \tag{3}$$

$$s_k = \bar{x}_k - x_k, \quad k = 0, \dots, q \tag{4}$$

$$t_k = \bar{y}_k - y_k, \quad k = 0, \dots, q \quad (5)$$

$$z_k^2 \geq w_k^2 + u_k^2, \quad k = 0, \dots, q \quad (6)$$

$$s_k^2 + t_k^2 \leq r_k^2, \quad k = 0, \dots, q \quad (7)$$

$$z_k \geq 0; w_k, u_k, s_k, t_k \text{ free} \quad k = 0, \dots, q \quad (8)$$

$$x_i, y_i \text{ free} \quad i = 0, \dots, q \quad (9)$$

In this SOCP formulation the objective function (1) is linear. The variable  $z_k, k = 0, \dots, q$ , represents the distance between subsequent vertices  $i_{k-1}$  and  $i_k$  in the partial sequence  $\mathcal{S}$ . The auxiliary variables  $w, u, s$  and  $t$  are defined in the linear constraints (2–5). They represent differences of coordinates used to calculate Euclidean distances. The Second-Order Cone (SOC) constraints (6) define the length of the edge connecting the subsequent customers from the sequence  $\mathcal{S}$ . The quadratic constraints (7) ensure that the *hitting points* will lie within their respective customers' covering circles. The expressions (8) and (9) are bounding constraints over the variables.

It is known that SOCP problems can be solved in polynomial time (Andersen et al. 2003). Furthermore, some well-known optimization softwares are also now capable of addressing this important class of problems.

### 3.2. Root relaxation

This section explains how the algorithm determines the initial sequence, i.e., the one generated at the root node.

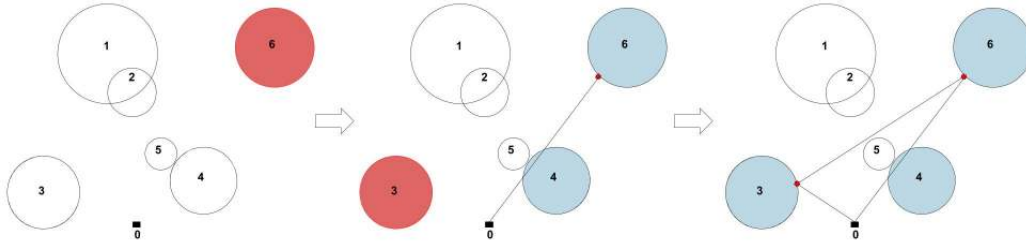
The three vertices from the initial sequence is selected as follows. The first vertex to be selected is the depot. In the CETSP instances proposed in the literature the radius of the depot is assumed to be zero. The next vertex to be chosen is the one that is most distant from the depot. The third vertex to be inserted is the one that leads to the largest lower bound value. More specifically, the algorithm solves a SOCP problem for all remaining candidates and selects the vertex associated to the sequence that yields the best relaxation.

Figure 5 illustrates an example involving 7 vertices. It can be observed that the depot (vertex 0) is the first vertex to be selected to be part of the sequence, followed by vertex 6 (the most distant from 0), and by vertex 3, whose insertion criterion is the one just mentioned above.

### 3.3. Checking feasibility

In this section we explain the procedure developed for checking if a certain branch-and-bound subproblem solution is feasible or not for the CETSP.

Let  $\hat{V}$  be a set of uncovered vertices and let  $\hat{d}_i$  be the distance between a vertex  $i \in \hat{V}$  and the edge of a subproblem solution that is nearest to  $i$ . Suppose that  $c$  and  $\overline{p_1 p_2}$  are an arbitrary vertex



**Figure 5** Example of the procedure to find a valid root relaxation

and an arbitrary edge of a partial solution. We are interested in determining the coordinates of a point  $p \in \overline{p_1 p_2}$  that minimizes the distance between  $\overline{p_1 p_2}$  and  $c$ .

The minimum distance  $\hat{d}$  between  $c$  and  $\overline{p_1 p_2}$  is computed by solving the optimization problem defined by Equation (10):

$$\hat{d} = \min_{0 \leq \theta \leq 1} \|(1 - \theta)p_1 + \theta p_2 - c\| \quad (10)$$

whose analytical solution to the unconstrained problem is given by  $\theta^* = -\frac{(p_2 - p_1)^\top (p_1 - c)}{\|p_2 - p_1\|^2}$ . Therefore, the minimum distance can be computed by Equation (11):

$$\hat{d} = \begin{cases} \|p_1 - c\|, & \text{if } \theta^* \leq 0 \\ \|p - c\|, & \text{if } 0 < \theta^* < 1, \text{ where } p = (1 - \theta^*)p_1 + \theta^* p_2 \\ \|p_2 - c\|, & \text{if } \theta^* \geq 1 \end{cases} \quad (11)$$

In order to check the feasibility of a subproblem solution one must compute the value of  $\hat{d}$  for every vertex, i.e. not in the current subsequence, and for every existent edge in this partial solution, compare with the corresponding disk radius. If  $\hat{d}$  is not greater than such radius, than the vertex is considered covered. If the number of vertices is given by  $u$  and the number of edges is given by  $v$  then this verification takes  $\mathcal{O}(uv)$  operations. Note that this approach allows for dealing with instances in  $\mathbb{R}^2$  or  $\mathbb{R}^3$ .

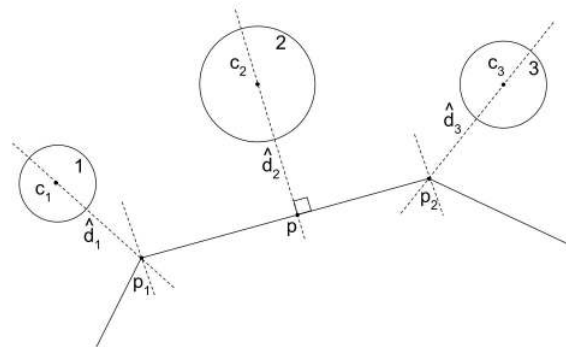


**Figure 6** Example involving an edge and three uncovered vertices of a partial CETSP solution

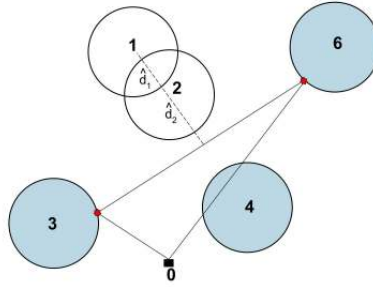


Figure 6 shows an example for three vertices and one edge. For vertex 1,  $\theta^* < 0$ , thus the minimum distance between  $c$  and  $\overline{p_1 p_2}$  is equal to the distance between  $c$  and  $p_1$ . For vertex 2,  $0 < \theta^* < 1$ , thus the minimum distance between  $c$  and  $\overline{p_1 p_2}$  is equal to the distance between  $c$  and  $p$ . Finally, for vertex 3,  $\theta^* > 1$ , thus the minimum distance between  $c$  and  $\overline{p_1 p_2}$  is equal to the distance between  $c$  and  $p_2$ .

### 3.4. Branching rules

In this section we describe the two branching criteria used to select a vertex to be inserted in a partial solution associated to a node of the branch-and-bound tree. The adequate criterion is automatically chosen based on the radii of the instances.

If all vertices have the same radius, the method proceed as follows. The algorithm first computes the value of  $\hat{d}_k$  for every  $k \in \hat{V}$ . Next, the maximum value among all  $\hat{d}_k$  is determined, that is,  $\max_{k \in \hat{V}} \{\hat{d}_k\}$ , and the corresponding vertex  $k$  is selected to be inserted in the partial solution. Figure 7 depicts an example of how the vertex selection is performed. In this case, we are given a partial solution  $0 \rightarrow 3 \rightarrow 6 \rightarrow 0$ . Note that vertex 4 is covered, but vertices 1 and 2 are not, thus  $\hat{V} = \{1, 2\}$ . It can be seen that  $\hat{d}_1 > \hat{d}_2$ . Hence, vertex 1 is the one associated to  $\max_{k \in \hat{V}} \{\hat{d}_k\}$ .



**Figure 7** Illustration of the branching rule used when all vertices have the same radius

If the vertices have different radii, the following schemed is used. At First, for all vertices  $k \in \hat{V}$ , the algorithm computes an estimative, given by  $\gamma_k$ , of how much the lower bound would increase if the vertex  $k$  were inserted between its closest neighbors in the sequence. In order to estimate  $\gamma_k$ , the procedure first calculates the coordinates of the point  $\tilde{p}_k$  on the border of the disk  $D_k$  that minimizes the distance between this point and its nearest edge  $\overline{p_1 p_2}$  on the sequence. Hence,  $\gamma_k$  can be computed as  $\gamma_k = \tilde{e}_1^k + \tilde{e}_2^k - e_{ij}$ , where  $\tilde{e}_1^k$  is the distance between  $\tilde{p}_k$  and  $p_1$ ,  $\tilde{e}_2^k$  is the distance between  $\tilde{p}_k$  and  $p_2$  and  $e_{ij}$  is the length of the edge  $\overline{p_1 p_2}$ . Figure 8 shows an example of this procedure, where  $\hat{V} = \{1, 2\}$ . Therefore  $\gamma_1 = \tilde{e}_1^1 + \tilde{e}_2^1 - e_{34}$  and  $\gamma_2 = \tilde{e}_1^2 + \tilde{e}_2^2 - e_{40}$ . Suppose that  $\gamma_2 > \gamma_1$ , as the figure suggest. Therefore, following the second branching rule, the vertex 2 is the one to be inserted in the sequence.

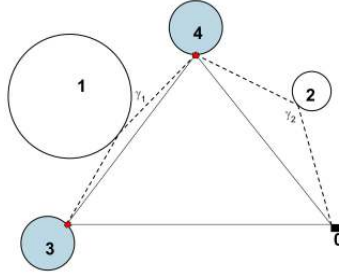


Figure 8 Illustration of the branching rule used when the vertices have different radii

#### 4. Computational experiments

The branch-and-bound algorithm was coded in C++ and the tests were carried out in an Intel Core i7 with 3.40 GHz and 16 GB of RAM running under Linux Mint 13. The SOCPs were solved using CPLEX 12.4. Only a single thread was used in our experiments. The 3D illustrations were generated using a MATLAB routine called *BUBBLEPLOT3* (Bodin 2009).

We performed a series of experiments to choose the most interesting branching strategy to be adopted. Tests were carried out using the following strategies: depth-first search, breadth-first search and best-first search. The results revealed that the best-first search turned out to be the most suitable strategy to be applied in our algorithm.

The proposed algorithm was tested in 824 instances that were suggested by Mennell (2009) and Behdani and Smith (2013). The difficulty of each instance is associated with the notion of *overlap ratio*, given by Mennell (2009), which is defined as the ratio between the mean of the radii of all vertices and the largest side ( $l_{max}$ ) of the rectangle that involve all vertices and their radii, i.e.,  $overlap\ ratio = \frac{(\sum_{i=0}^n r_i)/n}{l_{max}}$ .

Mennell (2009) presents the following classifications for his instances. Six problems whose names start with *team*, plus the instance *bonus1000* were denoted **Team Problems**. Those starting with *rotatingDiamonds*, *bubbles*, *concentricCircles*, plus the instance *chaoSigleDep* were gathered in the subset called **Geometric Problems**. Finally, the instances *d493*, *dsj1000*, *kroD100*, *lin318*, *pcb442*, *rat195* and *rd400* were generated from the TSPLIB and they were called **TSPLIB Problems**.

The instances of the groups Team Problems and Geometric Problems were generated with  $r_i = r, i = 0, \dots, n$ , and different overlap ratios that were not specified. The instances of the group TSPLIB Problems were generated with radii of three different sizes, i.e., with three overlap ratios, namely: 0.02, 0.10 and 0.30. Only the instances of the groups Team Problems and TSPLIB Problems have 3D versions. Mennell (2009) also provided two groups of instances denoted **Team Random Radius Problems** and **TSPLIB Random Radius Problems**, with 2D and 3D versions, with radii generated at random in such a way that  $r_i \neq r_j, \forall i, j \in V$ .

Behdani and Smith (2013) provided 240 2D test-problems with 7, 9, 11, 13, 15, 17, 19 and 21 vertices. These instances were generated as follows. The position  $(\bar{x}_i, \bar{y}_i), i \in V$ , of each vertex and

the depot  $i_0$  were selected at random in a limited space of 16 units of length and 10 units if width. The coverage area of all vertices was defined as a circumference with radius  $r$ . In their experiments, the authors used three radii, namely: 0.25, 0.50 and 1.00, thus obtaining three distinct groups with overlap ratios 0.015, 0.030 and 0.060, respectively.

#### 4.1. Results found for the small instances of Behdani and Smith (2013)

Table 1 shows a summary of the results found for the instances of Behdani and Smith (2013). In this table, *Group* denotes the 8 groups of instances divided into three different subgroups (*overlap ratios* = 0.015, 0.030, 0.060), *Group Size* shows the number of instances of each group, *#Opt.* indicates the number of optimal solutions obtained for each group, *Tree Size* corresponds to the average tree size and *Avg. Time* is the average time, in seconds.

Group	Group Size	#Opt.	Avg. Tree Size	Avg. Time
r = 0.25 and overlap = 0.0156				
CETSP-06	30	30	26	0.029
CETSP-08	30	30	51	0.062
CETSP-10	30	30	86	0.107
CETSP-12	30	30	139	0.189
CETSP-14	30	30	219	0.308
CETSP-16	30	30	443	0.673
CETSP-18	30	30	544	0.839
CETSP-20	30	30	1016	1.656
r = 0.50 and overlap = 0.0313				
CETSP-06	30	30	19	0.020
CETSP-08	30	30	39	0.047
CETSP-10	30	30	66	0.085
CETSP-12	30	30	92	0.125
CETSP-14	30	30	144	0.204
CETSP-16	30	30	222	0.334
CETSP-18	30	30	331	0.525
CETSP-20	30	30	437	0.719
r = 1.0 and overlap = 0.0625				
CETSP-06	30	30	13	0.017
CETSP-08	30	30	23	0.030
CETSP-10	30	30	38	0.049
CETSP-12	30	30	51	0.066
CETSP-14	30	30	71	0.100
CETSP-16	30	30	95	0.144
CETSP-18	30	30	117	0.176
CETSP-20	30	30	163	0.261

From Table 1, it can be observed the all instances were solved to optimality in a matter of seconds, as opposed to the method of Behdani and Smith (2013) whose lower/upper bounds were obtained in much higher computing time.

The complete results obtained by our branch-and-bound algorithm for the instances of Behdani and Smith (2013) can be found in Appendix.

#### 4.2. Results found for the 2D instances of Mennell (2009)

The results for the 2D instances of Mennell (2009) can be found in Table 2. In this table, *Instance* is the name of the instance,  $|V|$  indicates the size of the instance, *UB* denotes the upper bound obtained by Mennell (2009), *LB* is the lower bound by a given method, *Opt.* corresponds to the cost of the optimal solutions found by our branch-and-bound algorithm, *Tree Size* represents the size of the branch-and-bound tree, *Gap (%)* indicates the gap between the lower bound and the best known upper bound or the optimal solution, and *Time (s)* is the total computing time in seconds. It should be noted that a time limit of 4 hours was imposed for each instance. New improved (optimal) solutions are highlighted in boldface.

By observing the results of Table 2, we can see that our branch-and-bound algorithm was found capable of finding the optimal solutions of 22 out of 62 instances. We can also verify that all lower bounds available in the literature were dramatically improved. Moreover, the larger the overlap ratio, the better the algorithm behaves. This was somewhat expected since the number of vertices in the optimal tour tends to be inversely proportional to the overlap ratio value, thus helping the branch-and-bound algorithm to quickly converge towards an optimal solution, since less nodes are required to be explored throughout the tree.

Five new improved solutions were found and their associated optimal tours, as well as the one of the instance *team1\_100rdmRad*, are depicted in Figures 9-14.

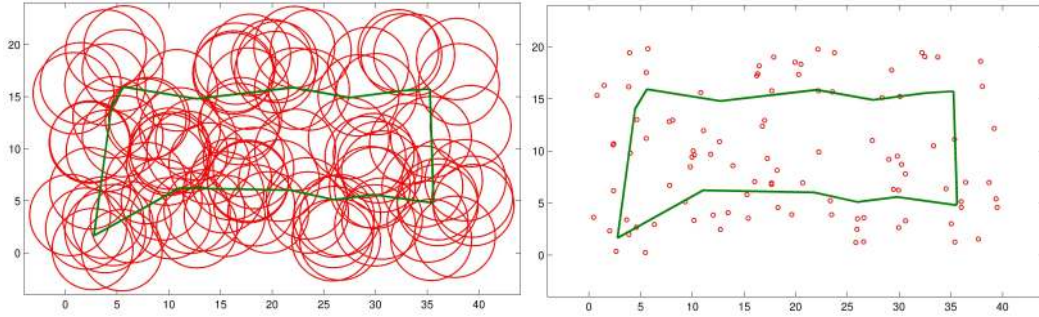
#### 4.3. Results found for the 3D instances of Mennell (2009)

Table 3 presents the results obtained for the 3D instances of Mennell (2009). The meaning of the columns in this table is the same as the one of the previous section. We can observe that our algorithm managed to find 10 optimal solutions, out of 42 instances. As it happened for the 2D instances, all lower bounds were improved.

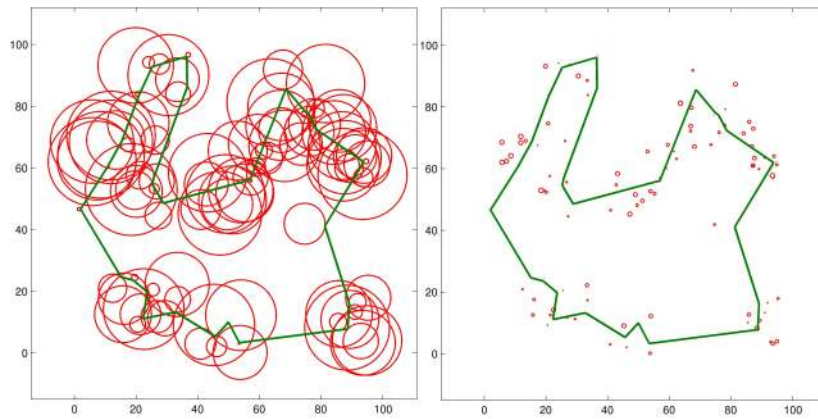
The branch-and-bound algorithm was found capable of improving 6 solutions and their associated optimal tours are shown in Figures 15-20.

Table 2 Results for 2D instances of Mennell

Instance	Size	Overlap ratio	Mennell (2009)		Branch and Bound				
			UB	LB	Opt.	LB	Tree Size	Gap (%)	Time (s)
<b>Low overlap ratio</b>									
d493	493	0.02	202.793	57.460	-	<b>146.331</b>	859216	27.842	14400.17
dsj1000	1000	0.02	935.743	100.190	-	<b>559.114</b>	585631	40.249	14400.24
kroD100	100	0.02	159.046	78.830	-	<b>142.872</b>	1784161	10.169	14400.16
lin318	318	0.02	2863.366	977.430	-	<b>1990.902</b>	933499	30.470	14400.08
pcb442	442	0.02	323.034	32.510	-	<b>185.847</b>	842855	42.468	14400.03
rat195	195	0.02	158.785	28.200	-	<b>108.104</b>	1108939	31.918	14400.04
rd400	400	0.02	1033.414	284.030	-	<b>567.190</b>	891890	45.115	14400.27
<b>Moderate overlap ratio</b>									
d493	493	0.10	101.735	31.730	<b>100.721</b>	<b>100.721</b>	8343	0.000	53.28
dsj1000	1000	0.10	376.099	10.170	-	<b>373.730</b>	718104	0.630	14400.51
kroD100	100	0.10	89.668	0.000	89.668	<b>89.668</b>	798	0.000	1.86
lin318	318	0.10	1408.482	0.000	<b>1394.626</b>	<b>1394.626</b>	1118666	0.000	8541.19
pcb442	442	0.10	147.244	1.870	-	<b>137.448</b>	1383948	6.653	14400.09
rat195	195	0.10	68.083	0.000	<b>67.991</b>	<b>67.991</b>	4735	0.000	17.32
rd400	400	0.10	466.102	0.000	-	<b>432.798</b>	1436555	7.145	14400.03
<b>High overlap ratio</b>									
d493	493	0.30	69.758	16.750	69.758	<b>69.758</b>	3	0.000	0.32
dsj1000	1000	0.30	199.948	0.000	199.948	<b>199.948</b>	17	0.000	0.75
kroD100	100	0.30	58.541	0.000	58.541	<b>58.541</b>	3	0.000	0.07
lin318	318	0.30	765.964	0.000	765.964	<b>765.964</b>	7	0.000	0.24
pcb442	442	0.30	83.537	0.000	83.537	<b>83.537</b>	3	0.000	0.31
rat195	195	0.30	45.702	0.000	45.702	<b>45.702</b>	3	0.000	0.13
rd400	400	0.30	224.839	0.000	224.839	<b>224.839</b>	24	0.000	0.33
<b>Varied overlap ratios</b>									
bonus1000	1001	0.12	402.470	0.000	-	<b>359.383</b>	949465	10.706	14400.02
bubbles1	37	0.07	349.135	60.620	349.135	<b>349.135</b>	66	0.000	0.10
bubbles2	77	0.06	428.279	60.620	428.279	<b>428.279</b>	121	0.000	0.22
bubbles3	127	0.06	530.733	60.620	<b>529.955</b>	<b>529.955</b>	31995	0.000	193.12
bubbles4	185	0.06	829.888	60.620	-	<b>690.578</b>	1502931	16.787	14400.01
bubbles5	251	0.05	1062.335	60.620	-	<b>851.822</b>	1181671	19.816	14400.28
bubbles6	325	0.05	1383.139	60.620	-	<b>993.981</b>	1025324	28.136	14400.15
bubbles7	407	0.05	1720.214	60.620	-	<b>1123.522</b>	918674	34.687	14400.19
bubbles8	497	0.05	2101.373	60.620	-	<b>1252.715</b>	894857	40.386	14400.28
bubbles9	595	0.04	2426.274	60.620	-	<b>1374.407</b>	765301	43.353	14400.33
chaoSingleDep	201	0.03	1039.610	439.260	-	<b>1000.151</b>	1760829	3.796	14400.09
concentricCircles1	17	0.03	53.158	14.000	53.158	<b>53.158</b>	2943	0.000	5.18
concentricCircles2	37	0.03	153.132	43.590	-	<b>149.868</b>	2699245	2.131	14400.03
concentricCircles3	61	0.02	271.076	115.280	-	<b>247.624</b>	2093145	8.651	14400.18
concentricCircles4	105	0.02	454.457	161.110	-	<b>358.887</b>	1320268	21.030	14400.06
concentricCircles5	149	0.02	645.381	249.980	-	<b>459.411</b>	1112726	28.815	14400.16
rotatingDiamonds1	21	0.02	32.389	6.200	32.389	<b>32.389</b>	59	0.000	0.09
rotatingDiamonds2	61	0.02	140.477	13.870	140.477	<b>140.477</b>	274967	0.000	730.37
rotatingDiamonds3	181	0.02	380.882	27.870	-	<b>348.608</b>	1612881	8.474	14400.07
rotatingDiamonds4	321	0.01	770.660	35.570	-	<b>593.350</b>	969457	23.008	14400.03
rotatingDiamonds5	681	0.01	1510.752	69.570	-	<b>1106.577</b>	777682	26.753	14400.23
team1_100	101	0.09	307.337	33.520	307.337	<b>307.337</b>	2805	0.000	9.61
team2_200	201	0.20	246.683	0.000	246.683	<b>246.683</b>	187	0.000	0.72
team3_300	301	0.07	466.241	8.750	-	<b>447.534</b>	1713428	4.012	14400.03
team4_400	401	0.05	680.211	20.590	-	<b>507.302</b>	938101	25.420	14400.10
team5_499	500	0.02	702.823	231.210	-	<b>524.589</b>	833603	25.360	14400.05
team6_500	501	0.27	225.216	0.000	225.216	<b>225.216</b>	24	0.000	0.43
<b>Arbitrary Radius Problems</b>									
bonus1000rdmRad	1001	0.06	987.114	-	-	<b>506.131</b>	656095	48.726	14400.22
d493rdmRad	493	0.13	140.120	-	-	<b>125.312</b>	1195835	10.568	14400.14
dsj1000rdmRad	1000	0.14	653.128	-	-	<b>509.740</b>	798273	21.954	14400.30
kroD100rdmRad	100	0.04	141.835	-	-	<b>136.620</b>	2293903	3.677	14400.12
lin318rdmRad	318	0.10	2080.574	-	-	<b>1807.681</b>	1349251	13.116	14400.00
pcb442rdmRad	442	0.09	235.188	-	-	<b>175.834</b>	966808	25.237	14400.23
rat195rdmRad	195	0.42	68.224	-	68.224	<b>68.224</b>	1628	0.000	5.16
rd400rdmRad	400	0.01	1252.380	-	-	<b>571.482</b>	776842	54.368	14400.29
team1_100rdmRad	101	0.08	388.537	-	388.537	<b>388.537</b>	86565	0.000	269.31
team2_200rdmRad	201	0.05	622.738	-	-	<b>488.182</b>	1098493	21.607	14400.12
team3_300rdmRad	301	0.24	381.828	-	<b>378.087</b>	<b>378.087</b>	132111	0.000	682.39
team4_400rdmRad	401	0.02	1011.772	-	-	<b>549.907</b>	870580	45.649	14400.32
team5_499rdmRad	500	0.20	454.327	-	-	<b>442.637</b>	1145471	2.573	14400.36
team6_500rdmRad	501	0.10	666.149	-	-	<b>489.612</b>	939270	26.501	14400.08



**Figure 9** Solution for *kroD100*, Equal radius, 2D, Size = 100, Length = 89.668



**Figure 10** Solution for *team1\_100rdmRad*, Arbitrary radius, 2D, Size = 101, Length = 388.537

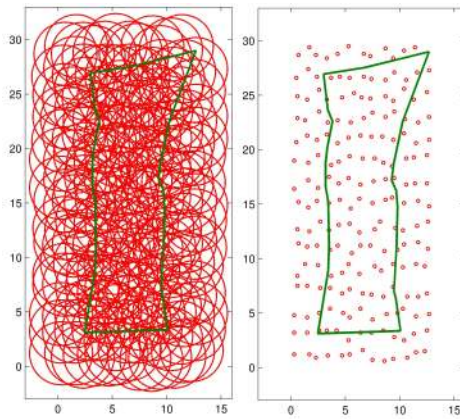


**Figure 11** Solution for *rat195*, Equal radius, 2D, Size = 195, Length = 67.991

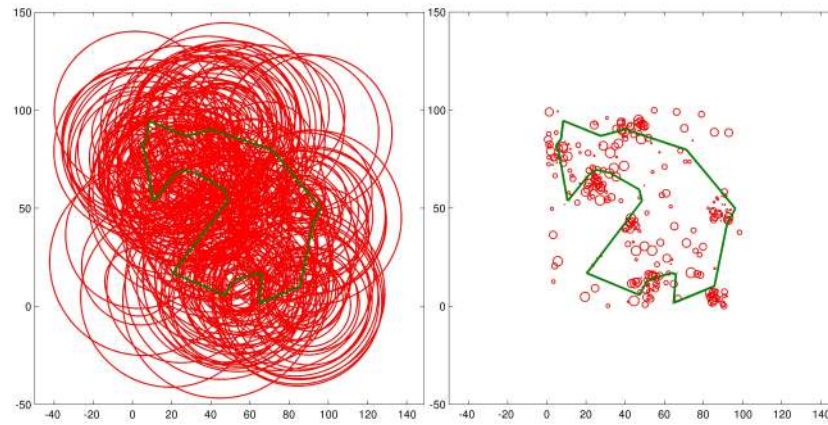


Figure 12 Solution for *team3\_300rdmRad*, Arbitrary radius, 2D, Size = 301, Length = 378.087

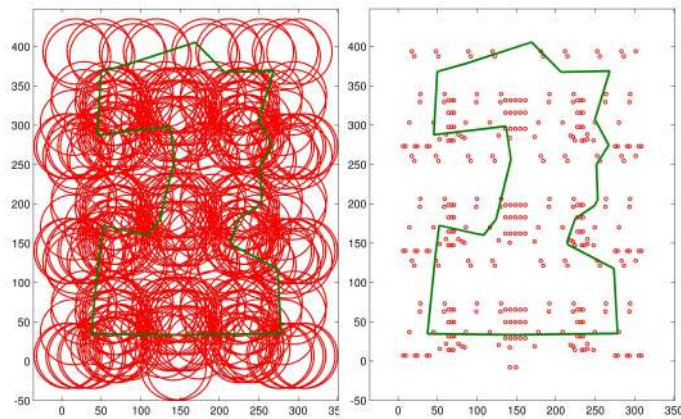


Figure 13 Solution for *lin318*, Equal radius, 2D, Size = 318, Length = 1394.626

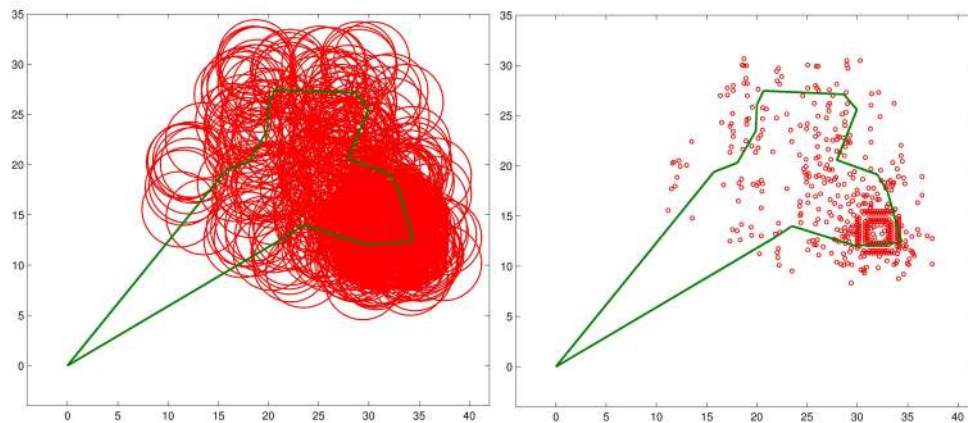


Figure 14 Solution for *d493*, Equal radius, 2D, Size = 493, Length = 100.721



Table 3 Results for 3D instances of Mennell

Instance	Size	Overlap ratio	Mennell (2009)		Branch and Bound				
			UB	LB	Opt.	LB	Tree Size	Gap (%)	Time (s)
<b>Low overlap ratio</b>									
d493	493	0.01	1353.137	-	-	<b>469.783</b>	642868	65.282	14400.01
dsj1000	1000	0.02	3147.865	-	-	<b>751.510</b>	494579	76.126	14400.05
kroD100	100	0.02	202.021	-	-	<b>148.231</b>	1183277	26.626	14400.12
lin318	318	0.02	3044.270	-	-	<b>1994.372</b>	934859	34.488	14400.14
pcb442	442	0.02	404.490	-	-	<b>186.381</b>	725462	53.922	14400.18
rat195	195	0.02	291.258	-	-	<b>126.493</b>	978598	56.570	14400.06
rd400	400	0.02	3218.198	-	-	<b>868.188</b>	753967	73.023	14400.12
<b>Moderate overlap ratio</b>									
d493	493	0.03	665.056	-	-	<b>421.164</b>	827584	36.672	14400.18
dsj1000	1000	0.10	1021.252	-	-	<b>602.987</b>	644546	40.956	14400.31
kroD100	100	0.10	91.669	-	<b>91.663</b>	<b>91.663</b>	2407	0.000	7.51
lin318	318	0.10	1443.427	-	-	<b>1398.254</b>	1588841	3.130	14400.12
pcb442	442	0.10	154.810	-	-	<b>137.951</b>	1209228	10.890	14400.13
rat195	195	0.10	112.405	-	-	<b>88.721</b>	1325338	21.070	14400.13
rd400	400	0.10	1552.723	-	-	<b>752.423</b>	851059	51.542	14400.24
<b>High overlap ratio</b>									
d493	493	0.08	335.592	-	<b>325.207</b>	<b>325.207</b>	5064	0.000	31.11
dsj1000	1000	0.30	270.399	-	<b>267.751</b>	<b>267.751</b>	2472	0.000	25.07
kroD100	100	0.30	58.926	-	58.926	<b>58.926</b>	4	0.000	0.08
lin318	318	0.30	766.831	-	766.831	<b>766.831</b>	8	0.000	0.24
pcb442	442	0.30	83.722	-	83.722	<b>83.722</b>	4	0.000	0.33
rat195	195	0.30	47.889	-	47.889	<b>47.889</b>	4	0.000	0.14
rd400	400	0.30	539.954	-	-	<b>450.720</b>	507442	16.526	14400.40
<b>Varied overlap ratios</b>									
bonus1000	1001	0.12	941.348	-	-	<b>472.559</b>	655479	49.800	14400.35
team1_100	101	0.09	820.727	-	-	<b>690.298</b>	1197716	15.892	14400.22
team2_200	201	0.20	283.238	-	<b>273.383</b>	<b>273.383</b>	86492	0.000	557.94
team3_300	301	0.07	1484.411	-	-	<b>762.683</b>	930319	48.620	14400.12
team4_400	401	0.05	753.813	-	-	<b>509.803</b>	894994	32.370	14400.30
team5_499	500	0.02	1924.527	-	-	<b>705.633</b>	665171	63.335	14400.20
team6_500	501	0.27	236.964	-	<b>230.923</b>	<b>230.923</b>	73	0.000	0.67
<b>Arbitrary Radius Problems</b>									
bonus1000rdmRad	1001	0.06	2689.413	-	-	<b>578.638</b>	512678	78.485	14400.04
d493rdmRad	493	0.03	761.065	-	-	<b>438.701</b>	858509	42.357	14400.06
dsj1000rdmRad	1000	0.14	2074.844	-	-	<b>696.289</b>	656155	66.441	14400.05
kroD100rdmRad	100	0.04	171.568	-	-	<b>137.765</b>	1350550	19.702	14400.13
lin318rdmRad	318	0.10	2189.426	-	-	<b>1806.783</b>	1200921	17.477	14400.10
pcb442rdmRad	442	0.09	258.404	-	-	<b>177.231</b>	962861	31.413	14400.09
rat195rdmRad	195	0.42	84.470	-	<b>82.105</b>	<b>82.105</b>	152636	0.000	790.53
rd400rdmRad	400	0.01	3592.601	-	-	<b>876.280</b>	766218	75.609	14400.06
team1_100rdmRad	101	0.08	907.593	-	-	<b>726.685</b>	1137079	19.933	14400.26
team2_200rdmRad	201	0.05	1055.948	-	-	<b>525.310</b>	1027597	50.252	14400.20
team3_300rdmRad	301	0.24	1053.380	-	-	<b>676.184</b>	1004637	35.808	14400.10
team4_400rdmRad	401	0.02	1276.896	-	-	<b>551.046</b>	793139	56.845	14400.08
team5_499rdmRad	500	0.20	840.477	-	-	<b>599.741</b>	940015	28.643	14400.28
team6_500rdmRad	501	0.10	1076.352	-	-	<b>507.122</b>	870473	52.885	14400.12



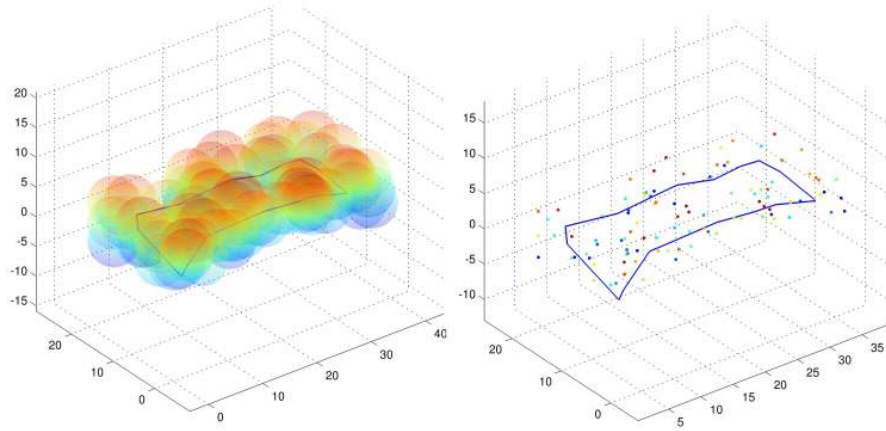


Figure 15 Solution for *kroD100*, Equal radius, 3D, Size = 100, Length = 91.663

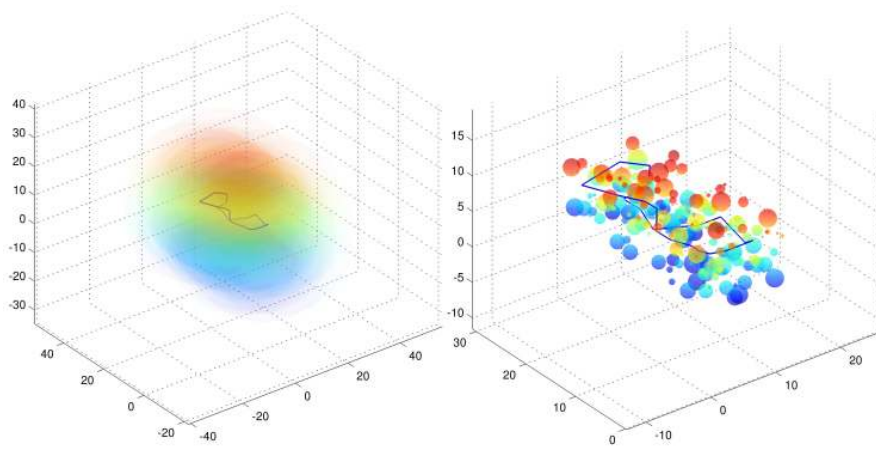


Figure 16 Solution for *rat195rdmRad*, Arbitrary radius, 3D, Size = 195, Length = 82.105

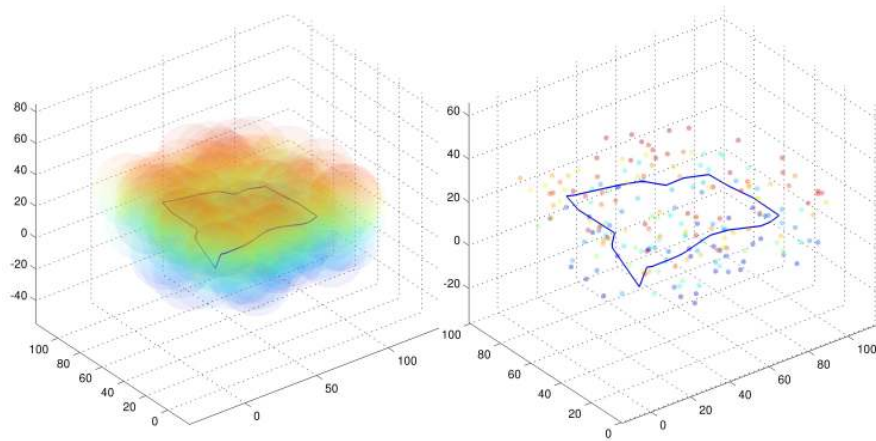


Figure 17 Solution for *team2\_200*, Equal radius, 3D, Size = 201, Length = 273.383

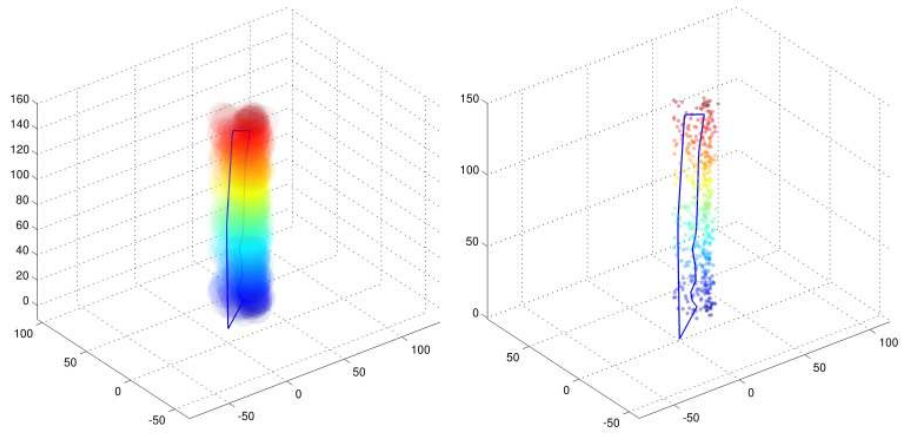


Figure 18 Solution for  $d_{493}$ , Equal radius, 3D, Size = 493, Length = 325.207

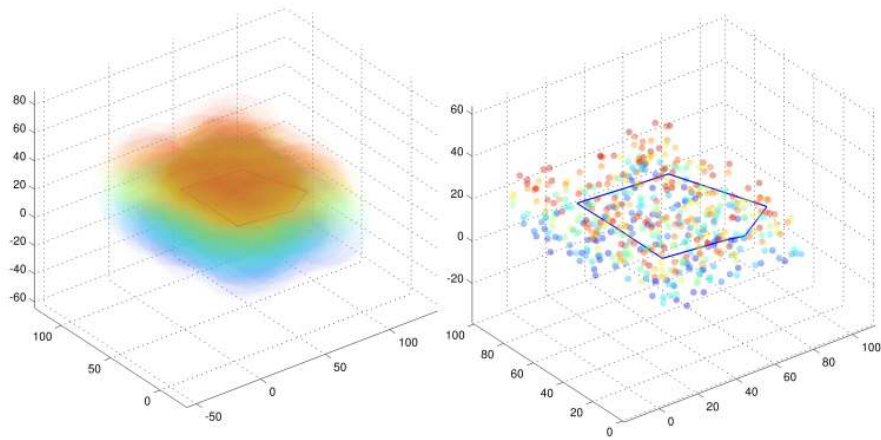


Figure 19 Solution for  $team6\_500$ , Equal radius, 3D, Size = 501, Length = 230.923

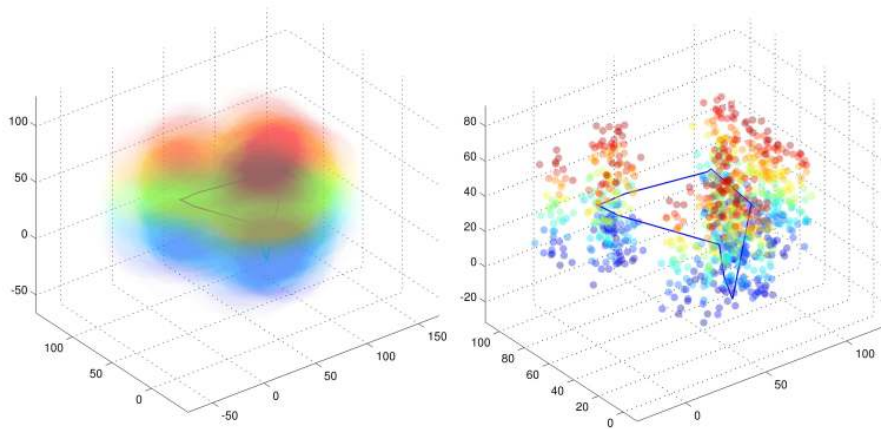


Figure 20 Solution for  $dsj1000$ , Equal radius, 3D, Size = 1000, Length = 267.751

## 5. Conclusions

This work presented a combinatorial branch-and-bound algorithm for the Close-Enough Traveling Salesman Problem (CETSP), where the subproblems solved in each node consists of a Second Order Cone Programming (SOCP). The proposed algorithm was tested in 824 instances available in the literature, namely: 720 two-dimensional instances suggested by Behdani and Smith (2013); 62 two-dimensional instances generated by Mennell (2009); and 42 three-dimensional instances developed by Mennell (2009). Our algorithm was found capable of obtaining the optimal solutions for 752 instances, more precisely, all 720 instances of Behdani and Smith (2013), 22 two-dimensional instances of Mennell (2009) and 10 three-dimensional instances of Mennell (2009). The lower bounds of all remaining instances were also improved.

The proposed algorithm performed quite well particularly on those instances with larger overlap ratios. In practical terms, these type of instances are more closely related with the technological advance. For example, better wireless transmitters and receptors tend to increase the coverage area of the equipments that use this type of technology, as in the case of AMR and other applications found in the literature, i.e., the radius of each vertex is likely to increase with the development of new technologies.

Promising avenues of research include the development of new approaches to improve the root relaxation, especially for smaller overlap ratios where the problem becomes closer to the classical TSP.

## **Acknowledgments**

The authors thank Dr. Manuel Iori for the valuable comments that helped improving the quality of the paper and Dr. Behdani and Dr. Smith for providing the instances generated in Behdani and Smith (2013).

**Appendix. Optimal solution found for instances of Behdani and Smith****(2013)**

**Table 4** Results for instances of Behdani,  $r = 0.25$ 

Instance	Size	Opt.	Tree Size	Time	Instance	Size	Opt.	Tree Size	Time
CETSP-6-0	7	28.051	33	0.04	CETSP-10-0	11	37.648	87	0.11
CETSP-6-1	7	33.862	33	0.04	CETSP-10-1	11	37.380	81	0.10
CETSP-6-2	7	27.641	21	0.02	CETSP-10-2	11	46.101	95	0.12
CETSP-6-3	7	25.392	33	0.03	CETSP-10-3	11	31.958	80	0.10
CETSP-6-4	7	36.758	21	0.02	CETSP-10-4	11	35.161	80	0.10
CETSP-6-5	7	22.151	16	0.02	CETSP-10-5	11	36.031	96	0.12
CETSP-6-6	7	27.903	27	0.03	CETSP-10-6	11	36.469	84	0.09
CETSP-6-7	7	34.763	16	0.02	CETSP-10-7	11	35.346	61	0.07
CETSP-6-8	7	24.165	33	0.04	CETSP-10-8	11	34.333	46	0.06
CETSP-6-9	7	28.473	27	0.03	CETSP-10-9	11	30.707	79	0.10
CETSP-6-10	7	34.718	21	0.02	CETSP-10-10	11	35.215	77	0.10
CETSP-6-11	7	31.599	27	0.03	CETSP-10-11	11	31.131	68	0.08
CETSP-6-12	7	33.352	33	0.04	CETSP-10-12	11	36.423	99	0.13
CETSP-6-13	7	26.710	21	0.02	CETSP-10-13	11	36.101	55	0.07
CETSP-6-14	7	28.679	33	0.04	CETSP-10-14	11	34.273	85	0.11
CETSP-6-15	7	34.118	16	0.02	CETSP-10-15	11	32.977	33	0.04
CETSP-6-16	7	23.635	33	0.03	CETSP-10-16	11	31.408	63	0.08
CETSP-6-17	7	22.834	16	0.02	CETSP-10-17	11	36.172	101	0.13
CETSP-6-18	7	28.359	21	0.03	CETSP-10-18	11	39.150	33	0.04
CETSP-6-19	7	33.198	21	0.02	CETSP-10-19	11	40.899	110	0.14
CETSP-6-20	7	34.851	32	0.04	CETSP-10-20	11	33.825	96	0.12
CETSP-6-21	7	32.084	33	0.04	CETSP-10-21	11	41.348	62	0.08
CETSP-6-22	7	27.746	21	0.02	CETSP-10-22	11	38.272	114	0.15
CETSP-6-23	7	29.058	33	0.04	CETSP-10-23	11	35.299	68	0.08
CETSP-6-24	7	33.151	21	0.02	CETSP-10-24	11	40.596	194	0.24
CETSP-6-25	7	30.280	21	0.02	CETSP-10-25	11	37.139	88	0.11
CETSP-6-26	7	30.264	33	0.04	CETSP-10-26	11	39.277	211	0.26
CETSP-6-27	7	30.783	32	0.04	CETSP-10-27	11	32.420	99	0.12
CETSP-6-28	7	35.940	21	0.02	CETSP-10-28	11	37.996	81	0.10
CETSP-6-29	7	41.384	33	0.03	CETSP-10-29	11	35.405	63	0.07
CETSP-8-0	9	32.069	63	0.08	CETSP-12-0	13	39.338	142	0.20
CETSP-8-1	9	35.697	52	0.06	CETSP-12-1	13	36.202	127	0.18
CETSP-8-2	9	25.439	27	0.03	CETSP-12-2	13	47.604	124	0.16
CETSP-8-3	9	37.387	63	0.08	CETSP-12-3	13	35.264	122	0.18
CETSP-8-4	9	29.294	47	0.06	CETSP-12-4	13	35.417	101	0.13
CETSP-8-5	9	33.514	47	0.06	CETSP-12-5	13	41.358	337	0.46
CETSP-8-6	9	25.672	61	0.07	CETSP-12-6	13	37.860	101	0.14
CETSP-8-7	9	30.022	39	0.04	CETSP-12-7	13	36.973	61	0.08
CETSP-8-8	9	33.499	47	0.06	CETSP-12-8	13	40.990	156	0.21
CETSP-8-9	9	38.936	47	0.06	CETSP-12-9	13	34.931	95	0.12
CETSP-8-10	9	30.246	21	0.02	CETSP-12-10	13	42.983	124	0.16
CETSP-8-11	9	29.826	47	0.06	CETSP-12-11	13	37.885	101	0.13
CETSP-8-12	9	33.321	33	0.04	CETSP-12-12	13	34.975	101	0.13
CETSP-8-13	9	30.726	45	0.05	CETSP-12-13	13	39.387	166	0.22
CETSP-8-14	9	36.420	68	0.08	CETSP-12-14	13	35.921	119	0.16
CETSP-8-15	9	32.921	59	0.07	CETSP-12-15	13	42.698	72	0.09
CETSP-8-16	9	36.022	47	0.06	CETSP-12-16	13	40.948	160	0.23
CETSP-8-17	9	31.365	40	0.05	CETSP-12-17	13	37.094	145	0.21
CETSP-8-18	9	32.128	33	0.04	CETSP-12-18	13	40.735	122	0.17
CETSP-8-19	9	35.199	62	0.08	CETSP-12-19	13	40.487	177	0.24
CETSP-8-20	9	30.768	47	0.06	CETSP-12-20	13	35.198	147	0.21
CETSP-8-21	9	33.503	55	0.07	CETSP-12-21	13	41.530	241	0.33
CETSP-8-22	9	41.536	63	0.07	CETSP-12-22	13	39.740	270	0.37
CETSP-8-23	9	34.153	63	0.08	CETSP-12-23	13	35.212	99	0.13
CETSP-8-24	9	33.788	63	0.08	CETSP-12-24	13	38.687	145	0.19
CETSP-8-25	9	39.793	68	0.08	CETSP-12-25	13	40.777	159	0.21
CETSP-8-26	9	37.755	55	0.06	CETSP-12-26	13	34.894	122	0.18
CETSP-8-27	9	35.772	68	0.09	CETSP-12-27	13	36.297	138	0.20
CETSP-8-28	9	31.315	52	0.07	CETSP-12-28	13	37.256	114	0.15
CETSP-8-29	9	34.974	47	0.05	CETSP-12-29	13	37.005	79	0.10

Table 5 Results for instances of Behdani,  $r = 0.25$ 

Instance	Size	Opt.	Tree Size	Time	Instance	Size	Opt.	Tree Size	Time
CETSP-14-0	15	40.445	209	0.32	CETSP-18-0	19	41.322	362	0.60
CETSP-14-1	15	41.751	231	0.31	CETSP-18-1	19	48.079	250	0.35
CETSP-14-2	15	40.154	388	0.62	CETSP-18-2	19	41.234	445	0.72
CETSP-14-3	15	36.239	123	0.18	CETSP-18-3	19	44.681	1259	1.94
CETSP-14-4	15	41.032	454	0.57	CETSP-18-4	19	44.842	238	0.40
CETSP-14-5	15	36.336	166	0.25	CETSP-18-5	19	40.794	211	0.33
CETSP-14-6	15	36.549	93	0.12	CETSP-18-6	19	40.294	798	1.10
CETSP-14-7	15	42.216	210	0.29	CETSP-18-7	19	38.894	173	0.28
CETSP-14-8	15	37.416	168	0.23	CETSP-18-8	19	35.898	140	0.19
CETSP-14-9	15	37.945	99	0.13	CETSP-18-9	19	37.798	264	0.44
CETSP-14-10	15	37.478	170	0.25	CETSP-18-10	19	44.962	295	0.46
CETSP-14-11	15	39.180	200	0.28	CETSP-18-11	19	50.117	722	1.18
CETSP-14-12	15	37.982	214	0.33	CETSP-18-12	19	44.023	354	0.55
CETSP-14-13	15	44.277	137	0.19	CETSP-18-13	19	43.899	507	0.78
CETSP-14-14	15	43.238	210	0.33	CETSP-18-14	19	45.635	1331	2.05
CETSP-14-15	15	41.829	165	0.26	CETSP-18-15	19	42.191	475	0.69
CETSP-14-16	15	45.761	226	0.30	CETSP-18-16	19	45.936	907	1.36
CETSP-14-17	15	36.990	461	0.64	CETSP-18-17	19	45.855	1068	1.66
CETSP-14-18	15	42.912	563	0.79	CETSP-18-18	19	46.274	319	0.48
CETSP-14-19	15	40.263	421	0.60	CETSP-18-19	19	43.434	290	0.44
CETSP-14-20	15	36.329	147	0.20	CETSP-18-20	19	43.548	270	0.38
CETSP-14-21	15	38.699	146	0.19	CETSP-18-21	19	38.735	1246	1.96
CETSP-14-22	15	42.718	307	0.42	CETSP-18-22	19	40.608	291	0.40
CETSP-14-23	15	40.349	102	0.14	CETSP-18-23	19	41.802	284	0.39
CETSP-14-24	15	41.446	137	0.18	CETSP-18-24	19	47.271	1011	1.66
CETSP-14-25	15	37.190	100	0.14	CETSP-18-25	19	45.342	272	0.44
CETSP-14-26	15	43.857	192	0.28	CETSP-18-26	19	47.429	404	0.65
CETSP-14-27	15	38.837	215	0.30	CETSP-18-27	19	43.228	381	0.65
CETSP-14-28	15	39.600	186	0.22	CETSP-18-28	19	42.901	684	1.11
CETSP-14-29	15	35.514	118	0.17	CETSP-18-29	19	46.983	1066	1.53
CETSP-16-0	17	40.875	261	0.40	CETSP-20-0	21	41.663	480	0.84
CETSP-16-1	17	46.802	140	0.20	CETSP-20-1	21	48.582	808	1.30
CETSP-16-2	17	38.612	286	0.44	CETSP-20-2	21	39.706	318	0.56
CETSP-16-3	17	43.401	213	0.32	CETSP-20-3	21	52.071	3147	5.32
CETSP-16-4	17	39.596	344	0.57	CETSP-20-4	21	42.449	541	0.88
CETSP-16-5	17	38.984	186	0.27	CETSP-20-5	21	46.030	479	0.72
CETSP-16-6	17	43.818	432	0.65	CETSP-20-6	21	47.124	996	1.52
CETSP-16-7	17	40.548	588	0.83	CETSP-20-7	21	42.608	313	0.54
CETSP-16-8	17	39.123	196	0.31	CETSP-20-8	21	41.654	712	1.12
CETSP-16-9	17	35.423	170	0.22	CETSP-20-9	21	46.386	419	0.70
CETSP-16-10	17	37.432	236	0.36	CETSP-20-10	21	46.776	1393	2.30
CETSP-16-11	17	41.860	336	0.54	CETSP-20-11	21	46.903	497	0.86
CETSP-16-12	17	52.277	374	0.55	CETSP-20-12	21	43.134	1173	2.01
CETSP-16-13	17	42.703	198	0.32	CETSP-20-13	21	45.156	1678	2.77
CETSP-16-14	17	46.434	288	0.39	CETSP-20-14	21	43.382	930	1.41
CETSP-16-15	17	41.872	1517	2.47	CETSP-20-15	21	43.001	541	0.88
CETSP-16-16	17	41.846	831	1.30	CETSP-20-16	21	46.982	917	1.45
CETSP-16-17	17	39.106	404	0.64	CETSP-20-17	21	44.101	356	0.54
CETSP-16-18	17	45.459	962	1.35	CETSP-20-18	21	46.090	397	0.66
CETSP-16-19	17	43.594	546	0.78	CETSP-20-19	21	44.669	3832	6.12
CETSP-16-20	17	46.199	340	0.48	CETSP-20-20	21	47.551	2155	3.52
CETSP-16-21	17	41.393	171	0.25	CETSP-20-21	21	43.062	392	0.62
CETSP-16-22	17	38.608	165	0.26	CETSP-20-22	21	46.051	740	1.22
CETSP-16-23	17	43.711	344	0.55	CETSP-20-23	21	48.816	2133	3.60
CETSP-16-24	17	40.266	2007	3.00	CETSP-20-24	21	47.472	413	0.73
CETSP-16-25	17	40.601	481	0.76	CETSP-20-25	21	46.423	1691	2.65
CETSP-16-26	17	41.155	247	0.36	CETSP-20-26	21	48.101	955	1.44
CETSP-16-27	17	45.308	320	0.51	CETSP-20-27	21	45.339	472	0.75
CETSP-16-28	17	44.838	306	0.44	CETSP-20-28	21	48.392	1365	2.29
CETSP-16-29	17	43.588	397	0.66	CETSP-20-29	21	42.662	245	0.37

**Table 6** Results for instances of Behdani,  $r = 0.50$ 

Instance	Size	Opt.	Tree Size	Time	Instance	Size	Opt.	Tree Size	Time
CETSP-6-0	7	27.164	21	0.02	CETSP-10-0	11	36.226	63	0.08
CETSP-6-1	7	32.438	16	0.02	CETSP-10-1	11	36.068	55	0.08
CETSP-6-2	7	26.227	16	0.02	CETSP-10-2	11	43.585	88	0.11
CETSP-6-3	7	23.935	21	0.02	CETSP-10-3	11	29.474	62	0.08
CETSP-6-4	7	35.406	21	0.02	CETSP-10-4	11	32.983	63	0.08
CETSP-6-5	7	20.845	21	0.02	CETSP-10-5	11	33.773	81	0.11
CETSP-6-6	7	26.733	11	0.01	CETSP-10-6	11	33.972	60	0.07
CETSP-6-7	7	33.762	7	0.01	CETSP-10-7	11	33.713	45	0.06
CETSP-6-8	7	23.139	16	0.02	CETSP-10-8	11	32.692	47	0.06
CETSP-6-9	7	26.858	21	0.02	CETSP-10-9	11	29.165	79	0.10
CETSP-6-10	7	33.643	3	0.00	CETSP-10-10	11	33.006	63	0.08
CETSP-6-11	7	30.132	27	0.03	CETSP-10-11	11	29.322	63	0.08
CETSP-6-12	7	31.772	21	0.02	CETSP-10-12	11	34.276	101	0.14
CETSP-6-13	7	25.305	21	0.02	CETSP-10-13	11	34.601	33	0.04
CETSP-6-14	7	27.151	16	0.02	CETSP-10-14	11	32.403	33	0.04
CETSP-6-15	7	33.025	16	0.02	CETSP-10-15	11	31.671	21	0.02
CETSP-6-16	7	22.020	16	0.02	CETSP-10-16	11	29.763	47	0.06
CETSP-6-17	7	21.703	11	0.01	CETSP-10-17	11	34.073	63	0.08
CETSP-6-18	7	27.068	21	0.02	CETSP-10-18	11	37.721	33	0.04
CETSP-6-19	7	32.157	21	0.02	CETSP-10-19	11	38.688	77	0.10
CETSP-6-20	7	33.252	32	0.04	CETSP-10-20	11	32.356	79	0.11
CETSP-6-21	7	30.580	33	0.04	CETSP-10-21	11	39.490	46	0.06
CETSP-6-22	7	26.557	21	0.02	CETSP-10-22	11	36.241	63	0.08
CETSP-6-23	7	28.093	21	0.02	CETSP-10-23	11	33.579	53	0.06
CETSP-6-24	7	31.733	21	0.02	CETSP-10-24	11	38.026	141	0.18
CETSP-6-25	7	29.335	7	0.01	CETSP-10-25	11	35.192	63	0.08
CETSP-6-26	7	28.663	21	0.02	CETSP-10-26	11	36.788	161	0.22
CETSP-6-27	7	28.979	32	0.03	CETSP-10-27	11	30.414	80	0.10
CETSP-6-28	7	34.603	11	0.01	CETSP-10-28	11	36.087	64	0.08
CETSP-6-29	7	39.621	21	0.02	CETSP-10-29	11	33.712	63	0.08
CETSP-8-0	9	30.944	16	0.02	CETSP-12-0	13	37.472	120	0.17
CETSP-8-1	9	34.073	47	0.06	CETSP-12-1	13	34.105	87	0.12
CETSP-8-2	9	24.006	33	0.04	CETSP-12-2	13	45.216	96	0.13
CETSP-8-3	9	35.591	47	0.06	CETSP-12-3	13	33.168	72	0.10
CETSP-8-4	9	27.767	47	0.06	CETSP-12-4	13	33.247	63	0.08
CETSP-8-5	9	31.987	27	0.03	CETSP-12-5	13	38.045	207	0.29
CETSP-8-6	9	24.419	39	0.05	CETSP-12-6	13	36.152	72	0.10
CETSP-8-7	9	27.828	40	0.06	CETSP-12-7	13	35.054	61	0.08
CETSP-8-8	9	31.971	21	0.03	CETSP-12-8	13	38.392	135	0.19
CETSP-8-9	9	37.380	33	0.04	CETSP-12-9	13	32.537	72	0.10
CETSP-8-10	9	28.967	21	0.02	CETSP-12-10	13	40.701	109	0.15
CETSP-8-11	9	28.288	47	0.06	CETSP-12-11	13	35.910	63	0.08
CETSP-8-12	9	31.521	33	0.04	CETSP-12-12	13	33.445	51	0.06
CETSP-8-13	9	28.872	33	0.04	CETSP-12-13	13	36.958	100	0.13
CETSP-8-14	9	34.467	68	0.08	CETSP-12-14	13	33.757	80	0.10
CETSP-8-15	9	31.669	47	0.06	CETSP-12-15	13	40.832	47	0.06
CETSP-8-16	9	34.394	33	0.04	CETSP-12-16	13	38.250	101	0.14
CETSP-8-17	9	30.064	21	0.02	CETSP-12-17	13	35.078	81	0.11
CETSP-8-18	9	30.813	33	0.04	CETSP-12-18	13	38.755	80	0.10
CETSP-8-19	9	33.528	63	0.08	CETSP-12-19	13	38.255	126	0.18
CETSP-8-20	9	29.178	33	0.04	CETSP-12-20	13	32.621	135	0.20
CETSP-8-21	9	31.785	33	0.04	CETSP-12-21	13	38.628	101	0.14
CETSP-8-22	9	40.239	16	0.01	CETSP-12-22	13	36.827	147	0.20
CETSP-8-23	9	32.256	47	0.05	CETSP-12-23	13	32.797	79	0.10
CETSP-8-24	9	32.332	47	0.06	CETSP-12-24	13	36.264	95	0.13
CETSP-8-25	9	38.023	46	0.06	CETSP-12-25	13	38.079	79	0.10
CETSP-8-26	9	35.871	47	0.05	CETSP-12-26	13	33.076	79	0.11
CETSP-8-27	9	34.183	52	0.06	CETSP-12-27	13	34.343	89	0.12
CETSP-8-28	9	29.566	47	0.06	CETSP-12-28	13	35.105	77	0.10
CETSP-8-29	9	33.382	47	0.06	CETSP-12-29	13	35.301	60	0.08



Table 7 Results for instances of Behdani,  $r = 0.50$ 

Instance	Size	Opt.	Tree Size	Time	Instance	Size	Opt.	Tree Size	Time
CETSP-14-0	15	38.144	145	0.20	CETSP-18-0	19	38.647	203	0.34
CETSP-14-1	15	38.897	102	0.14	CETSP-18-1	19	44.777	167	0.27
CETSP-14-2	15	36.873	224	0.36	CETSP-18-2	19	38.075	274	0.42
CETSP-14-3	15	34.153	81	0.11	CETSP-18-3	19	41.214	793	1.30
CETSP-14-4	15	37.938	266	0.35	CETSP-18-4	19	41.760	197	0.33
CETSP-14-5	15	34.309	80	0.11	CETSP-18-5	19	38.092	150	0.23
CETSP-14-6	15	34.163	94	0.13	CETSP-18-6	19	37.199	661	0.97
CETSP-14-7	15	39.126	138	0.19	CETSP-18-7	19	36.395	147	0.23
CETSP-14-8	15	34.576	155	0.22	CETSP-18-8	19	33.670	109	0.16
CETSP-14-9	15	36.029	101	0.14	CETSP-18-9	19	34.848	152	0.23
CETSP-14-10	15	34.984	124	0.18	CETSP-18-10	19	41.544	145	0.22
CETSP-14-11	15	36.633	98	0.14	CETSP-18-11	19	46.029	324	0.53
CETSP-14-12	15	35.211	109	0.16	CETSP-18-12	19	40.859	181	0.27
CETSP-14-13	15	42.163	78	0.10	CETSP-18-13	19	40.881	424	0.71
CETSP-14-14	15	39.660	172	0.27	CETSP-18-14	19	42.097	1089	1.71
CETSP-14-15	15	38.956	120	0.18	CETSP-18-15	19	39.184	342	0.53
CETSP-14-16	15	43.036	129	0.18	CETSP-18-16	19	42.831	854	1.40
CETSP-14-17	15	34.118	361	0.51	CETSP-18-17	19	41.837	408	0.64
CETSP-14-18	15	39.138	193	0.28	CETSP-18-18	19	43.036	124	0.18
CETSP-14-19	15	37.169	232	0.33	CETSP-18-19	19	40.200	191	0.30
CETSP-14-20	15	33.705	129	0.19	CETSP-18-20	19	40.761	218	0.33
CETSP-14-21	15	36.001	114	0.16	CETSP-18-21	19	35.102	665	1.18
CETSP-14-22	15	40.335	293	0.41	CETSP-18-22	19	37.855	208	0.29
CETSP-14-23	15	37.776	96	0.14	CETSP-18-23	19	38.742	152	0.22
CETSP-14-24	15	38.901	100	0.14	CETSP-18-24	19	43.602	495	0.82
CETSP-14-25	15	35.315	80	0.11	CETSP-18-25	19	42.263	146	0.22
CETSP-14-26	15	41.050	142	0.20	CETSP-18-26	19	44.130	118	0.18
CETSP-14-27	15	35.670	96	0.14	CETSP-18-27	19	39.536	195	0.32
CETSP-14-28	15	37.160	178	0.23	CETSP-18-28	19	38.639	293	0.50
CETSP-14-29	15	33.382	81	0.11	CETSP-18-29	19	43.128	515	0.73
CETSP-16-0	17	38.275	201	0.33	CETSP-20-0	21	38.739	258	0.46
CETSP-16-1	17	43.809	122	0.19	CETSP-20-1	21	45.003	327	0.52
CETSP-16-2	17	35.349	172	0.26	CETSP-20-2	21	35.925	272	0.50
CETSP-16-3	17	40.967	145	0.22	CETSP-20-3	21	47.701	1063	1.74
CETSP-16-4	17	36.532	185	0.30	CETSP-20-4	21	38.803	334	0.58
CETSP-16-5	17	36.325	127	0.18	CETSP-20-5	21	42.775	436	0.70
CETSP-16-6	17	40.611	276	0.41	CETSP-20-6	21	43.403	452	0.70
CETSP-16-7	17	36.929	389	0.58	CETSP-20-7	21	39.752	257	0.47
CETSP-16-8	17	36.339	169	0.26	CETSP-20-8	21	38.485	287	0.44
CETSP-16-9	17	33.331	114	0.15	CETSP-20-9	21	42.688	193	0.31
CETSP-16-10	17	34.640	135	0.21	CETSP-20-10	21	42.292	424	0.72
CETSP-16-11	17	38.621	140	0.20	CETSP-20-11	21	43.559	236	0.36
CETSP-16-12	17	48.726	149	0.22	CETSP-20-12	21	39.616	628	1.10
CETSP-16-13	17	40.540	111	0.16	CETSP-20-13	21	40.837	550	0.91
CETSP-16-14	17	43.490	174	0.22	CETSP-20-14	21	39.776	393	0.58
CETSP-16-15	17	38.138	632	0.95	CETSP-20-15	21	39.736	365	0.59
CETSP-16-16	17	38.114	317	0.49	CETSP-20-16	21	43.453	483	0.75
CETSP-16-17	17	35.580	216	0.37	CETSP-20-17	21	40.772	208	0.31
CETSP-16-18	17	41.865	426	0.61	CETSP-20-18	21	42.364	232	0.40
CETSP-16-19	17	40.260	255	0.36	CETSP-20-19	21	40.147	1180	1.91
CETSP-16-20	17	43.267	182	0.26	CETSP-20-20	21	43.641	718	1.18
CETSP-16-21	17	38.757	97	0.13	CETSP-20-21	21	40.437	223	0.33
CETSP-16-22	17	36.616	80	0.12	CETSP-20-22	21	42.471	468	0.80
CETSP-16-23	17	40.556	206	0.32	CETSP-20-23	21	44.577	709	1.23
CETSP-16-24	17	36.057	724	1.08	CETSP-20-24	21	44.272	281	0.52
CETSP-16-25	17	37.188	166	0.27	CETSP-20-25	21	42.111	722	1.14
CETSP-16-26	17	38.817	186	0.26	CETSP-20-26	21	44.167	417	0.64
CETSP-16-27	17	41.874	184	0.29	CETSP-20-27	21	41.926	324	0.55
CETSP-16-28	17	41.669	177	0.26	CETSP-20-28	21	44.357	474	0.80
CETSP-16-29	17	40.348	209	0.35	CETSP-20-29	21	39.296	200	0.32

Table 8 Results for instances of Behdani,  $r = 1.0$ 

Instance	Size	Opt.	Tree Size	Time	Instance	Size	Opt.	Tree Size	Time
CETSP-6-0	7	25.492	21	0.03	CETSP-10-0	11	33.676	47	0.06
CETSP-6-1	7	30.070	7	0.01	CETSP-10-1	11	33.975	22	0.03
CETSP-6-2	7	23.583	7	0.01	CETSP-10-2	11	39.391	45	0.06
CETSP-6-3	7	21.242	7	0.01	CETSP-10-3	11	25.712	21	0.03
CETSP-6-4	7	32.872	11	0.02	CETSP-10-4	11	29.385	47	0.06
CETSP-6-5	7	18.328	33	0.04	CETSP-10-5	11	30.549	33	0.04
CETSP-6-6	7	24.583	11	0.01	CETSP-10-6	11	29.905	52	0.06
CETSP-6-7	7	31.874	7	0.01	CETSP-10-7	11	31.081	16	0.02
CETSP-6-8	7	21.429	7	0.01	CETSP-10-8	11	30.131	21	0.03
CETSP-6-9	7	24.651	3	0.01	CETSP-10-9	11	26.385	72	0.10
CETSP-6-10	7	31.547	3	0.01	CETSP-10-10	11	29.958	27	0.04
CETSP-6-11	7	27.599	7	0.01	CETSP-10-11	11	25.754	46	0.06
CETSP-6-12	7	28.757	21	0.02	CETSP-10-12	11	31.008	52	0.06
CETSP-6-13	7	22.859	11	0.02	CETSP-10-13	11	31.673	33	0.04
CETSP-6-14	7	24.410	7	0.01	CETSP-10-14	11	29.243	16	0.02
CETSP-6-15	7	30.915	21	0.02	CETSP-10-15	11	29.146	21	0.02
CETSP-6-16	7	19.410	3	0.00	CETSP-10-16	11	26.944	33	0.04
CETSP-6-17	7	19.719	3	0.01	CETSP-10-17	11	30.583	47	0.06
CETSP-6-18	7	24.642	21	0.02	CETSP-10-18	11	35.006	18	0.03
CETSP-6-19	7	30.289	1	0.01	CETSP-10-19	11	35.341	33	0.04
CETSP-6-20	7	30.112	21	0.02	CETSP-10-20	11	29.807	16	0.03
CETSP-6-21	7	27.666	33	0.04	CETSP-10-21	11	36.794	21	0.03
CETSP-6-22	7	24.699	11	0.02	CETSP-10-22	11	33.030	55	0.07
CETSP-6-23	7	26.323	21	0.02	CETSP-10-23	11	30.539	47	0.06
CETSP-6-24	7	29.251	11	0.01	CETSP-10-24	11	33.796	63	0.08
CETSP-6-25	7	27.683	3	0.01	CETSP-10-25	11	31.857	33	0.04
CETSP-6-26	7	25.540	21	0.02	CETSP-10-26	11	32.308	78	0.11
CETSP-6-27	7	25.691	32	0.04	CETSP-10-27	11	27.130	58	0.08
CETSP-6-28	7	32.081	11	0.02	CETSP-10-28	11	32.835	25	0.03
CETSP-6-29	7	36.183	21	0.02	CETSP-10-29	11	31.368	33	0.04
CETSP-8-0	9	28.952	16	0.02	CETSP-12-0	13	34.781	40	0.04
CETSP-8-1	9	31.040	40	0.05	CETSP-12-1	13	31.290	15	0.02
CETSP-8-2	9	21.442	11	0.02	CETSP-12-2	13	41.043	63	0.08
CETSP-8-3	9	32.872	11	0.02	CETSP-12-3	13	29.392	47	0.06
CETSP-8-4	9	25.130	22	0.03	CETSP-12-4	13	29.861	33	0.04
CETSP-8-5	9	29.458	7	0.01	CETSP-12-5	13	32.559	120	0.18
CETSP-8-6	9	22.370	21	0.03	CETSP-12-6	13	34.125	7	0.01
CETSP-8-7	9	24.883	16	0.02	CETSP-12-7	13	31.965	47	0.06
CETSP-8-8	9	29.024	16	0.02	CETSP-12-8	13	34.148	80	0.11
CETSP-8-9	9	34.773	21	0.03	CETSP-12-9	13	28.670	63	0.08
CETSP-8-10	9	26.870	7	0.01	CETSP-12-10	13	36.543	70	0.09
CETSP-8-11	9	25.265	47	0.06	CETSP-12-11	13	32.700	39	0.05
CETSP-8-12	9	29.043	21	0.02	CETSP-12-12	13	30.844	37	0.05
CETSP-8-13	9	25.410	33	0.04	CETSP-12-13	13	33.012	67	0.09
CETSP-8-14	9	30.538	69	0.08	CETSP-12-14	13	30.262	33	0.04
CETSP-8-15	9	29.667	33	0.04	CETSP-12-15	13	37.461	33	0.04
CETSP-8-16	9	31.628	16	0.02	CETSP-12-16	13	34.406	33	0.04
CETSP-8-17	9	27.788	11	0.02	CETSP-12-17	13	32.065	33	0.04
CETSP-8-18	9	28.266	33	0.04	CETSP-12-18	13	35.911	33	0.04
CETSP-8-19	9	30.907	21	0.03	CETSP-12-19	13	34.633	63	0.08
CETSP-8-20	9	26.556	21	0.03	CETSP-12-20	13	29.612	63	0.08
CETSP-8-21	9	29.067	33	0.04	CETSP-12-21	13	34.539	46	0.06
CETSP-8-22	9	37.842	12	0.02	CETSP-12-22	13	32.308	78	0.11
CETSP-8-23	9	28.988	27	0.03	CETSP-12-23	13	29.230	47	0.06
CETSP-8-24	9	29.801	7	0.01	CETSP-12-24	13	31.748	81	0.11
CETSP-8-25	9	34.837	46	0.06	CETSP-12-25	13	34.127	62	0.08
CETSP-8-26	9	32.499	33	0.04	CETSP-12-26	13	29.896	32	0.04
CETSP-8-27	9	31.435	26	0.03	CETSP-12-27	13	30.937	60	0.08
CETSP-8-28	9	26.912	16	0.02	CETSP-12-28	13	31.753	54	0.07
CETSP-8-29	9	31.118	7	0.01	CETSP-12-29	13	32.269	47	0.06

Table 9 Results for instances of Behdani,  $r = 1.0$ 

Instance	Size	Opt.	Tree Size	Time	Instance	Size	Opt.	Tree Size	Time
CETSP-14-0	15	34.891	63	0.09	CETSP-18-0	19	35.121	63	0.09
CETSP-14-1	15	34.924	33	0.04	CETSP-18-1	19	39.579	91	0.14
CETSP-14-2	15	32.633	47	0.06	CETSP-18-2	19	32.945	101	0.15
CETSP-14-3	15	31.126	47	0.06	CETSP-18-3	19	35.849	170	0.24
CETSP-14-4	15	32.846	87	0.12	CETSP-18-4	19	37.675	47	0.06
CETSP-14-5	15	31.186	47	0.06	CETSP-18-5	19	34.073	86	0.12
CETSP-14-6	15	30.177	78	0.11	CETSP-18-6	19	31.038	300	0.47
CETSP-14-7	15	34.487	79	0.11	CETSP-18-7	19	32.758	47	0.07
CETSP-14-8	15	29.768	112	0.16	CETSP-18-8	19	30.074	63	0.09
CETSP-14-9	15	33.177	21	0.03	CETSP-18-9	19	31.082	54	0.07
CETSP-14-10	15	30.981	72	0.10	CETSP-18-10	19	36.530	98	0.15
CETSP-14-11	15	32.312	81	0.12	CETSP-18-11	19	40.579	146	0.22
CETSP-14-12	15	30.852	63	0.08	CETSP-18-12	19	36.199	99	0.15
CETSP-14-13	15	38.265	46	0.06	CETSP-18-13	19	35.674	191	0.28
CETSP-14-14	15	35.034	81	0.11	CETSP-18-14	19	35.797	189	0.29
CETSP-14-15	15	35.122	81	0.12	CETSP-18-15	19	34.262	108	0.16
CETSP-14-16	15	38.485	64	0.09	CETSP-18-16	19	36.065	215	0.34
CETSP-14-17	15	29.067	158	0.24	CETSP-18-17	19	35.929	131	0.21
CETSP-14-18	15	33.622	80	0.11	CETSP-18-18	19	38.803	47	0.07
CETSP-14-19	15	32.327	98	0.14	CETSP-18-19	19	36.045	87	0.13
CETSP-14-20	15	29.732	72	0.10	CETSP-18-20	19	36.313	96	0.14
CETSP-14-21	15	32.089	80	0.12	CETSP-18-21	19	29.907	81	0.12
CETSP-14-22	15	35.956	91	0.13	CETSP-18-22	19	33.977	172	0.24
CETSP-14-23	15	33.998	59	0.08	CETSP-18-23	19	33.849	101	0.15
CETSP-14-24	15	34.632	54	0.08	CETSP-18-24	19	37.888	200	0.34
CETSP-14-25	15	32.228	47	0.06	CETSP-18-25	19	37.034	91	0.14
CETSP-14-26	15	36.858	84	0.11	CETSP-18-26	19	39.959	33	0.05
CETSP-14-27	15	31.327	47	0.07	CETSP-18-27	19	35.011	63	0.09
CETSP-14-28	15	32.964	115	0.16	CETSP-18-28	19	32.906	135	0.22
CETSP-14-29	15	30.086	47	0.07	CETSP-18-29	19	36.725	200	0.30
CETSP-16-0	17	34.891	63	0.09	CETSP-20-0	21	35.182	80	0.12
CETSP-16-1	17	39.564	63	0.09	CETSP-20-1	21	39.549	81	0.12
CETSP-16-2	17	30.317	54	0.08	CETSP-20-2	21	31.125	101	0.16
CETSP-16-3	17	36.763	109	0.16	CETSP-20-3	21	41.023	225	0.36
CETSP-16-4	17	32.754	61	0.09	CETSP-20-4	21	33.327	147	0.24
CETSP-16-5	17	32.136	101	0.14	CETSP-20-5	21	36.919	184	0.32
CETSP-16-6	17	35.219	212	0.31	CETSP-20-6	21	37.616	185	0.29
CETSP-16-7	17	30.988	208	0.36	CETSP-20-7	21	35.581	91	0.13
CETSP-16-8	17	32.571	47	0.06	CETSP-20-8	21	33.817	103	0.16
CETSP-16-9	17	30.038	33	0.05	CETSP-20-9	21	37.473	79	0.11
CETSP-16-10	17	31.029	63	0.09	CETSP-20-10	21	35.743	192	0.33
CETSP-16-11	17	34.141	79	0.12	CETSP-20-11	21	38.366	137	0.22
CETSP-16-12	17	43.595	101	0.16	CETSP-20-12	21	34.488	321	0.52
CETSP-16-13	17	37.177	63	0.09	CETSP-20-13	21	34.494	157	0.26
CETSP-16-14	17	38.259	73	0.12	CETSP-20-14	21	34.645	135	0.20
CETSP-16-15	17	32.576	169	0.27	CETSP-20-15	21	34.790	163	0.22
CETSP-16-16	17	32.729	118	0.18	CETSP-20-16	21	37.822	189	0.30
CETSP-16-17	17	30.857	101	0.17	CETSP-20-17	21	36.094	109	0.16
CETSP-16-18	17	36.428	180	0.27	CETSP-20-18	21	36.882	146	0.24
CETSP-16-19	17	35.113	95	0.14	CETSP-20-19	21	32.868	197	0.31
CETSP-16-20	17	38.367	101	0.16	CETSP-20-20	21	38.084	276	0.44
CETSP-16-21	17	34.724	55	0.08	CETSP-20-21	21	35.649	166	0.28
CETSP-16-22	17	33.343	46	0.08	CETSP-20-22	21	36.922	154	0.25
CETSP-16-23	17	36.513	101	0.15	CETSP-20-23	21	38.927	254	0.45
CETSP-16-24	17	29.977	118	0.18	CETSP-20-24	21	40.088	97	0.15
CETSP-16-25	17	32.967	63	0.09	CETSP-20-25	21	35.367	250	0.42
CETSP-16-26	17	34.358	130	0.20	CETSP-20-26	21	38.045	139	0.21
CETSP-16-27	17	36.953	112	0.17	CETSP-20-27	21	36.404	356	0.62
CETSP-16-28	17	36.534	100	0.14	CETSP-20-28	21	38.698	86	0.13
CETSP-16-29	17	36.786	21	0.03	CETSP-20-29	21	34.393	86	0.12

## References

- Andersen, E. D., C. Roos, T. Terlaky. 2003. On implementing a primal-dual interior-point method for conic quadratic optimization. *Math. Programming* **95**(2) 249–277.
- Applegate, D. L., R. E. Bixby, V. Chvátal, W. J. Cook. 2011. *The Traveling Salesman Problem: A Computational Study (Princeton Series in Applied Mathematics)*. Princeton University Press.
- Arkin, E., R. Hassin. 1994. Approximation Algorithms For The Geometric Covering Salesman Problem. *Discrete Applied Mathematics* **55**(3) 197–218.
- Behdani, B., J. C. Smith. 2013. An Integer-Programming-Based Approach to the Close-Enough Traveling Salesman Problem. *INFORMS J. Comput.* Forthcoming.
- Bodin, Peter. 2009. BUBBLEPLOT3: A simple 3D bubbleplot. <http://www.mathworks.com/matlabcentral/fileexchange/8231-bubbleplot3>.
- Boyd, S., L. Vandenberghe. 2004. *Convex Optimization*. Cambridge University Press.
- Dong, J., N. Yang, M. Chen. 2007. Heuristic Approaches for a TSP Variant: The Automatic Meter Reading Shortest Tour Problem. *Extending the Horizons: Advances in Computing, Optimization, and Decision Technologies*, vol. 37. Springer US, 145–163.
- Farid, A., D. Goldfarb. 2003. Second-order cone programming. *Math. Programming* **95** 3–51.
- Gendreau, M., G. Laporte, F. Semet. 1997. The Covering Tour Problem. *Oper. Res.* **45**(4) 568–576.
- Gulczynski, D. J., J. W. Heath, C. C. Price. 2006. The Close Enough Traveling Salesman Problem: A Discussion of Several Heuristics. *Perspectives in Operations Research*, vol. 36. Springer US, 271–283.
- Hà, M. H., N. Bostel, A. Langevin, L. Rousseau. 2013. Solving the close-enough arc routing problem. *Networks* Forthcoming.
- Lobo, M.S., L. Vandenberghe, S. Boyd, H. Lebrete. 1998. Applications of second-order cone programming. *Linear Algebra Appl.* **284**(1-3) 193–228.
- Mennell, W. 2009. Heuristics for solving three routing problems: Close-Enough Traveling Salesman Problem, Close-Enough Vehicle Routing Problem, Sequence-Dependent Team Orienteering Problem. Ph.D. thesis, University of Maryland, College Park.
- Mennell, W., B. Golden, E. Wasil. 2011. A Steiner-Zone Heuristic for Solving the Close-Enough Traveling Salesman Problem. *12th INFORMS Computing Society Conference: Operations Research, Computing, and Homeland Defense*. Monterey, California.
- Shuttleworth, R., B. Golden, S. Smith, E. Wasil. 2008. Advances in Meter Reading: Heuristic Solution of the Close Enough Traveling Salesman Problem over a Street Network. *The Vehicle Routing Problem: Latest Advances and New Challenges*, vol. 43. 487–501.
- Silberholz, J., B. Golden. 2007. The Generalized Traveling Salesman Problem: A New Genetic Algorithm Approach. *Extending the Horizons: Advances in Computing, Optimization, and Decision Technologies*, vol. 37. Springer US, 165–181.

Yuan, B., M. Orlowska, S. Sadiq. 2007. On the optimal robot routing problem in wireless sensor networks. *IEEE Transactions on Knowledge and Data Engineering* **19**(9) 1252–1261.